Analysis of the densification of a vibrated sand packing

Ahmed Raihane, Olivier Bonnefoy, Jean-Marc Chaix, Jean-Louis Gelet, Gérard Thomas

Analysis of the densification of a vibrated sand packing

Ahmed Raihane[(1)], Olivier Bonnefoy*[(1)], Jean-Marc Chaix†[(2)], Jean-Louis Gelet[(3)], Gérard Thomas‡[(1)]

(1) Ecole Nationale Supérieure des Mines de Saint-Etienne, Centre SPIN, Département PMMC ; LPMG UMR CNRS 5148. ; 158, Cours Fauriel. 42023 Saint-Etienne Cedex 2, France.

(2) SIMAP-LTPCM, INPGrenoble-CNRS-UJF. BP 75 ; Domaine Universitaire 38402 Saint-Martin d'Hères, France

(3) Ferraz-Shawmut 6, rue de Vaucanson 69720 Saint-Bonnet de Mure, France.

Abstract

Two techniques have been used to analyse the densification of a silica sand by horizontal sinusoidal vibrations of frequency f = 50Hz for relative accelerations between 0 and 6: the quantitative analysis of motion observed through the transparent wall, and the altitude map of the free top surface of the sample. The first technique was used to analyse the transient regime: during the first 10 seconds, slight densification occurs at the bottom of the powder bed, while the upper part enters convective motion and the intermediate part reaches densities higher than 66%. The second technique allowed to quantify the evolution of the overall density *vs.* acceleration Γ during the steady regime (dynamic density) and after the vibrations (relaxed density): a maximum of density is observed in both cases for an optimal acceleration which depends on the initial height of the powder bed. These results are analyzed and discussed.

Keywords:

Sand granular medium ; horizontal vibrations ; densification ; image analysis

Introduction

Densification of granular media by horizontal vibrations is used in different applications at various scales and in various conditions. The present work is motivated by its application in the manufacturing process of high intensity electrical fuses developed by the Ferraz-Shawmut company. These devices are made of a ceramic box containing a silver fuse and filled up with sand grains. The electrical properties of the fuses strongly depend on the granular packing that needs to be compact and homogeneous. Horizontal vibrations are used to achieve this result.

A lot of experimental and theoretical works have been dedicated to the study of vertical vibrations on various granular materials [1-5] including silica sands for fuse fillers [6], but lower attention has been paid to horizontal vibrations. 2D studies have been performed, experimentally on disks [7], by computer simulations of single slices of spheres assumed to represent a "vertical cross section of a 3D sample" [8], or both experimentally and by computer simulation on a monolayer of glass spheres in a channel [9]. A few 3D experimental works, in boxes with length L_x (parallel to vibrations), L_y, and pile height H large with respect to the particle diameter d have also been published [10-12]. Various phenomena are observed and studied such as convective flow [4, 12, 13], transition from a solid-like state to a fluid-like state [11, 13, 14, 15], size separation [16] and surface patterns [17, 18,19]. Few studies investigated the bulk density evolution with the vibration parameters [20-22].

All these works deal with sinusoidal solicitations $x(t) = A\sin(2\pi ft)$ and generally admit that the relevant control parameter is the relative non dimensional acceleration:

$$\Gamma = (2\pi f)^2 A/g \qquad (1)$$

* obonnefoy@emse.fr,
† jean-marc.chaix@simap.grenoble-inpg.fr
‡ gthomas@emse.fr

where g is the gravity acceleration. Despite this agreement, the question of the actually relevant scaling parameters remains widely open. It is also clear that these parameters are correlated in a given experiment: for instance, in an experiment at given frequency f, A and Γ are related by Equation (1).

Two main phenomena have been evidenced:

- the "fluidization transition": at a critical relative acceleration Γ_1, the behaviour of a part of the granular sample switches from solid-like to fluid-like type. Fluidization is associated to an expansion of the granular medium in the fluidized region. In previous works [13, 22], we also considered the onset of densification which occurs at an acceleration Γ_0 below Γ_1.
- the convective motions in the sample above this critical value, giving rise to one, two or more convective rolls on the top part of the powder bed.

The qualitative behaviour of the bed with respect to acceleration Γ as deduced in particular from our previous studies [13, 22] is summarized on Figure 1: above the onset of densification, three regions of the bed are observed: an upper one, showing convection rolls, a bottom region considered as jammed, showing almost no densification, and an intermediate "glassy" one, in which densification is expected to be enhanced. For increasing accelerations, the fluidized region expands and tends to concern the whole sample. It must be noticed that for large enough accelerations, the sample tends to expand, due to the low density in the fluidized part.

In the present paper, attention is focused on densification processes with acceleration as control parameter, on the basis of two complementary approaches: the measurement of overall density from accurate evaluation of the sand bed volume, during and after vibrations, and the evaluation of bed settling observed along the box wall perpendicular to the vibration axis.

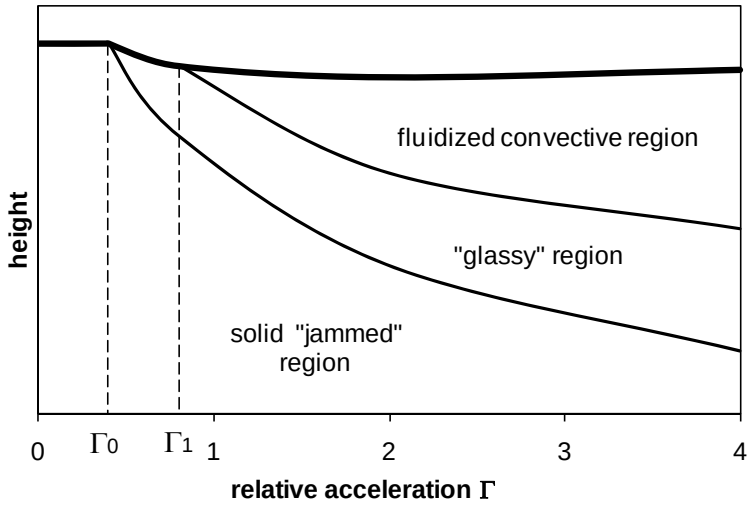

Figure 1: Schematic representation of the evolution of the (dynamic) sample height vs. relative acceleration Γ, showing the transitions at critical accelerations Γ_i. The upper curve shows the height of the sand pile. For $\Gamma>\Gamma_1$ above the fluidization transition of the top region, the top region is fluidized, while the other ones remain solid-like. Densification occurs either in the whole solid-like region, or in an intermediate "glassy" region.

Experimental setup and materials

Experimental device for vibrations

The experimental device has been described in [13]. It consists in a mobile horizontal table, on which a container is fixed and partly filled in with the granular material (Figure 2). The electromagnetic shaker Tira (TV51110) delivers a sinusoïdal vibration of controlled frequency f. The amplitude A is monitored by a power amplifier (Tira BAA 120) associated with a sinusoidal vibration control system (Ling Dynamic Systems DSC4). Coupled with a piezoelectric accelerometer (Bruel & Kjaer 4371 V) attached to the vibrating table, the control system adapts the amplitude A to the chosen acceleration Γ. In this study, the feed-back loop is deactivated, so that the target acceleration is reached within approximately 1 second. The sand container is a transparent Plexiglas box, which enables the observation through the walls during and after vibrations. The faces of the box parallel to the vibration axis are referred to as

East/West ones, whereas the perpendicular ones are referred to as North/South (Figure 2). An ultra-fast CCD camera records the grain flow on the North face.

In the present paper, a large box, L_x=40 mm, L_y=80 mm, L_z=80 mm was stuck to the vibrating table.

Most of the experiments reported in the present papers have been performed at f =50 Hz on samples with 60 mm initial height, and for relative acceleration Γ between 0 and 8.

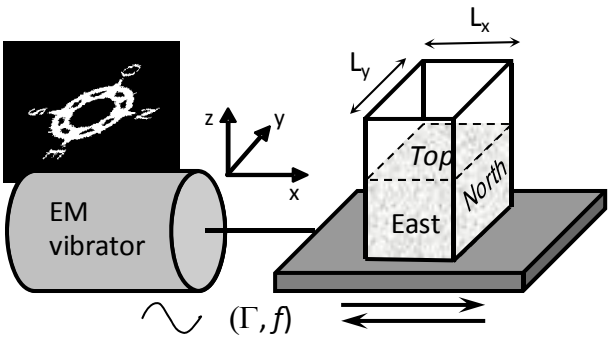

Figure 2: Experimental setup for horizontal vibrations

Granular Material

The physical characteristics of the grains (density, grain size, friction...) can play an important part, which, to some extent, could explain apparent contradictions between experiments by different authors in former works. The grain material is silica sand with more than 99% of alpha-quartz and a density of 2660 kg/m^3. The size distribution shows a moderate polydisperse material and a mean diameter of $d_{4,3}$=517 µm, with a narrow size distribution. The grains have a regular rounded shape (Figure 3). No internal close porosity has been detected: the pycnometer density determination shows that the grain density corresponds to the crystal one.

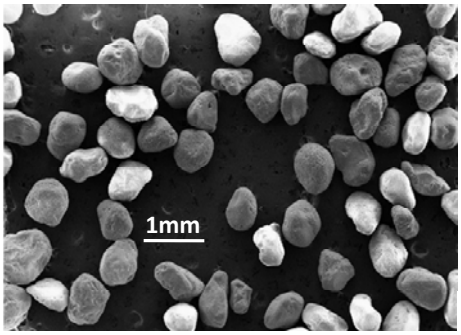

Figure 3: Silica sand: rounded shape grains with a narrow size distribution.

Initial packing of powders

Two protocols have been used to prepare granular beds with an homogeneous structure and a specified packing fraction.

The first protocol leads to a density of approximately 61.5%. It consists in pouring sand grains into the container directly from a funnel (min. diameter of 5 mm) situated ~50 mm above the free surface. During the filling, the funnel is moved here and there to form an almost plane sand bed. A small excess of sand grains is poured then removed by a Hoover® at constant level, related to a table vacuum cleaner. The final granular packing height is 60 mm. When followed carefully, this protocol ensures a reproducible and relatively low density as well as a good homogeneity of the packing.

The second protocol leads to a density of approximately 68%. It consists in pouring the sand grains over a mesh (aperture of 2 mm) situated ~100 mm above the free surface. This way, grains fall with a controlled velocity and are uniformly spread over the container surface (uniform rain) rather than flowing out of a localized source. This rain-like technique is known to lead to dense and homogeneous compact packings [23]. In the present work, it was only used here in some particular cases.

Characterisation techniques

Velocity measurements on the North face of the vibrating box

The ultra-fast camera recorded images of the grains situated along the transparent North face. An image analysis method based on optical flow conservation has been developed to measure the local motion or velocity field. This method computes an estimation of the apparent motion (velocity) of objects within an image sequence. For each pair of consecutive images, the local displacement of small areas is calculated on a grid of points (Figure 4). The method has been validated in different configurations: pure translation and pure rotation for numerical deformation or physical deformation (noise due to lighting fluctuations) [25]. The technique only needs that the two consecutive images correspond to a relatively small deformations of the structure.

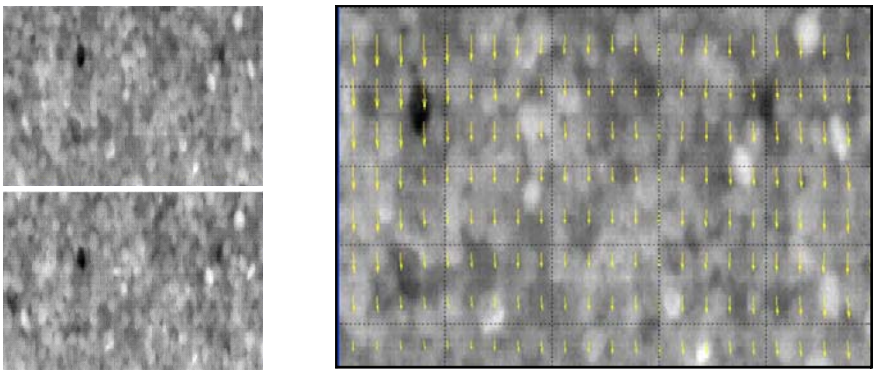

a b

Figure 4: Illustration of the local motion (velocity) measurements: two successive images of a region of the North face of the sample (a) and corresponding velocity field (b) calculated and plotted on a grid of points. The downward motion in this case is not homogeneous

The first application of the technique consists in evaluating the velocity fields, when stationary convection rolls are established: the analysis of velocity maps on images of the North face enables for instance to evaluate the limit between convective and glassy regions (Figure 2), and therefore the height of the convective region at any acceleration Γ [22, 25].

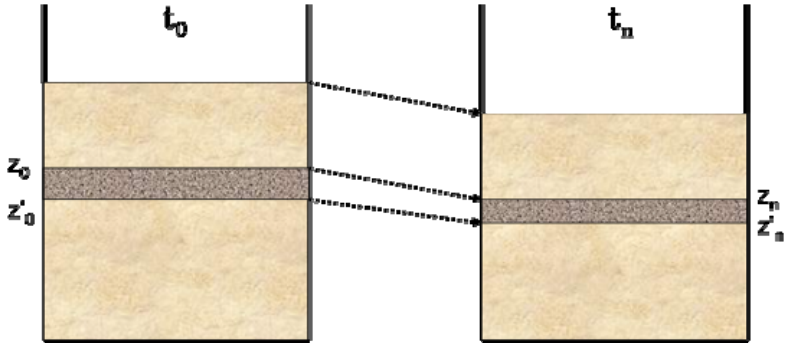

Figure 5: Schematic representation of the settling of the sample during the transient regime in the first seconds of vibration. The grey region moves downwards ("settling": decrease of z) and its width z'-z is reduced, which measures densification.

In the present paper, the technique is used in a different way, to evaluate the absolute settling of the sample during the transient regime. In this stage, a densification is generally observed: each layer of sand at a given height z_0 moves downwards (Figure 5).

The image analysis technique allows to measure the deformation field of the granular packing during a reasonably small time step. By integrating it iteratively through the whole vibration process, it is possible to compute the final altitude of a grain at any initial altitude. If we further assume that the grains movements are purely vertical during the settling (no inwards motion), the mass conservation may be written and this gives access to the final density. For a supposedly homogeneous initial state ($C=C_0$ for any altitude), the density profile is given by:

$$C(z_n) = \frac{C_0}{\left(\frac{\partial g}{\partial z}\right)_{z_0,t_n}} \qquad (2)$$

where $z_n = g(z_0,t_n)$ is the altitude at time t_n of the grain initially at altitude z_0.

The technique is of course limited to regions, where the motion is slow and corresponds to densification only: the results are quite biased in the upper part of the sample when convective motion is present.

Density measurements by integration of optical pen height measurements

In order to accurately measure the global density, a topographical analysis of the free surface is performed with a chromatic confocal imaging technique (STIL CHR150-OP24000). An optical pen (Figure 6a) placed 20 cm above the top of the sample is driven by a computer controlled motors so that the beam scans the sample on parallel lines. The measurement of the surface profile $z=f(x,y)$ can be done at rest as well as under vibrations in the stationary regime, with an accuracy on the z coordinate better than one grain diameter. The volume under the surface leads to a very accurate evaluation of the overall density of the sample.

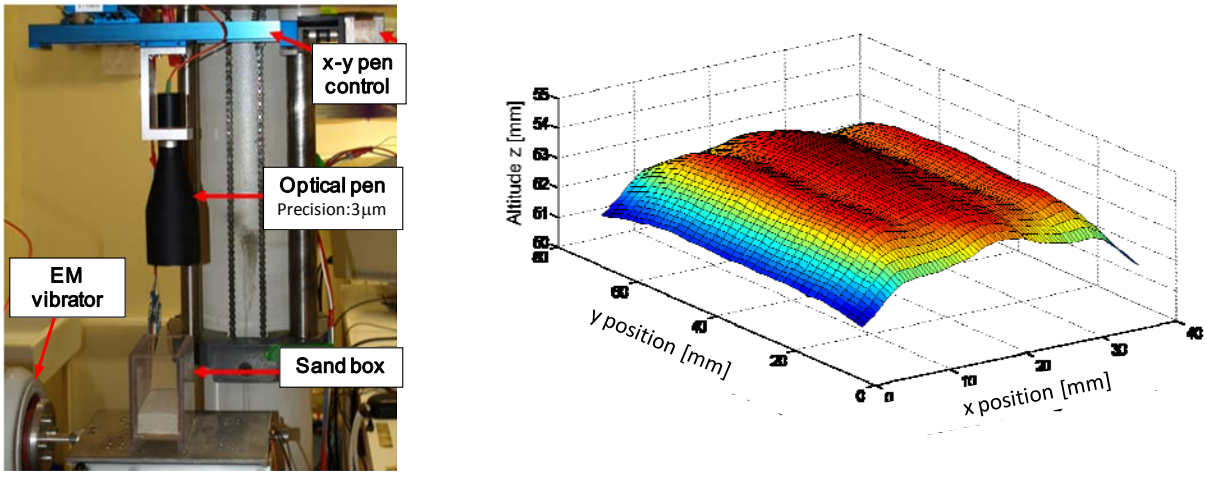

a b

Figure 6: Optical pen height measurement of the sand pile top surface profile. The optical pen is driven by an x-y table (a) so that the light beam scans the top of the sample line by line, always in the same direction (b). The surface profile (c) is obtained on a grid with typically 2 mm resolution in x and y, and better than 0.5 mm in z.

Experimental results

Transient regime

During the first 3 to 10 seconds after the beginning of vibrations, a transient regime is observed, where the mean sample height varies. For low acceleration, densification occurs inside the powder bed in a way which depends on altitude z. For larger times, the overall shape is stabilized, and only convective motion is observed in the upper part of the sample (for $\Gamma>\Gamma_1$). In this section, we present the results of densification as a function of altitude z and acceleration Γ, as measured by the above described technique from series of images on the North wall of the sample during vibrations. The range of studied values of acceleration is here limited to 0-4: for larger accelerations, the strong and complex sand motion inside the box prevents quantitative settling measurements.

The settling profiles $\delta z = g(z,t_n) - z$ *vs.* z are plotted in Figure 7 for t_n=3 sec. For small accelerations (Γ=0.7), the motion concerns only a 20 mm thick surface layer of the sample. For larger accelerations the settling progresses towards lower altitudes. It must be reminded that the slope $\left(\frac{\partial g}{\partial z}\right)$ of the curves corresponds to a densification rate (Equation 2), so that a curve with a constant slope (which is

roughly the case above z=4 mm for Γ=3 on Figure 7) corresponds to an homogeneous densification. For large enough accelerations (typically Γ>1) settling can be observed on the whole sample, except maybe for a very small region close to the bottom.

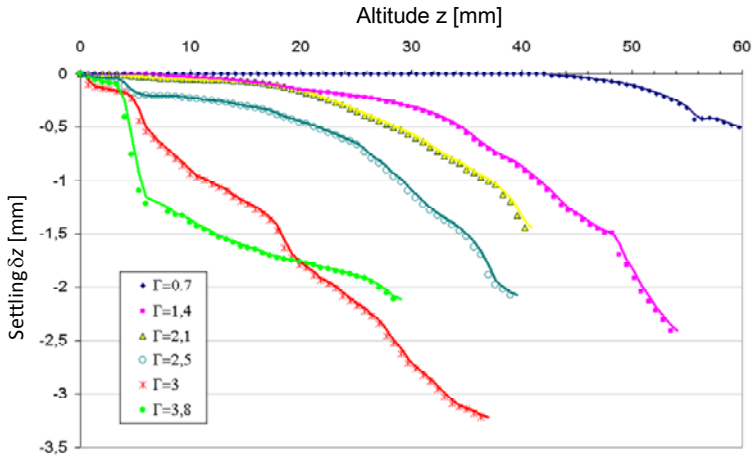

Figure 7: Settling profiles $\delta z = g(z,t_n) - z$ *vs. altitude z after 3 seconds for different accelerations.*

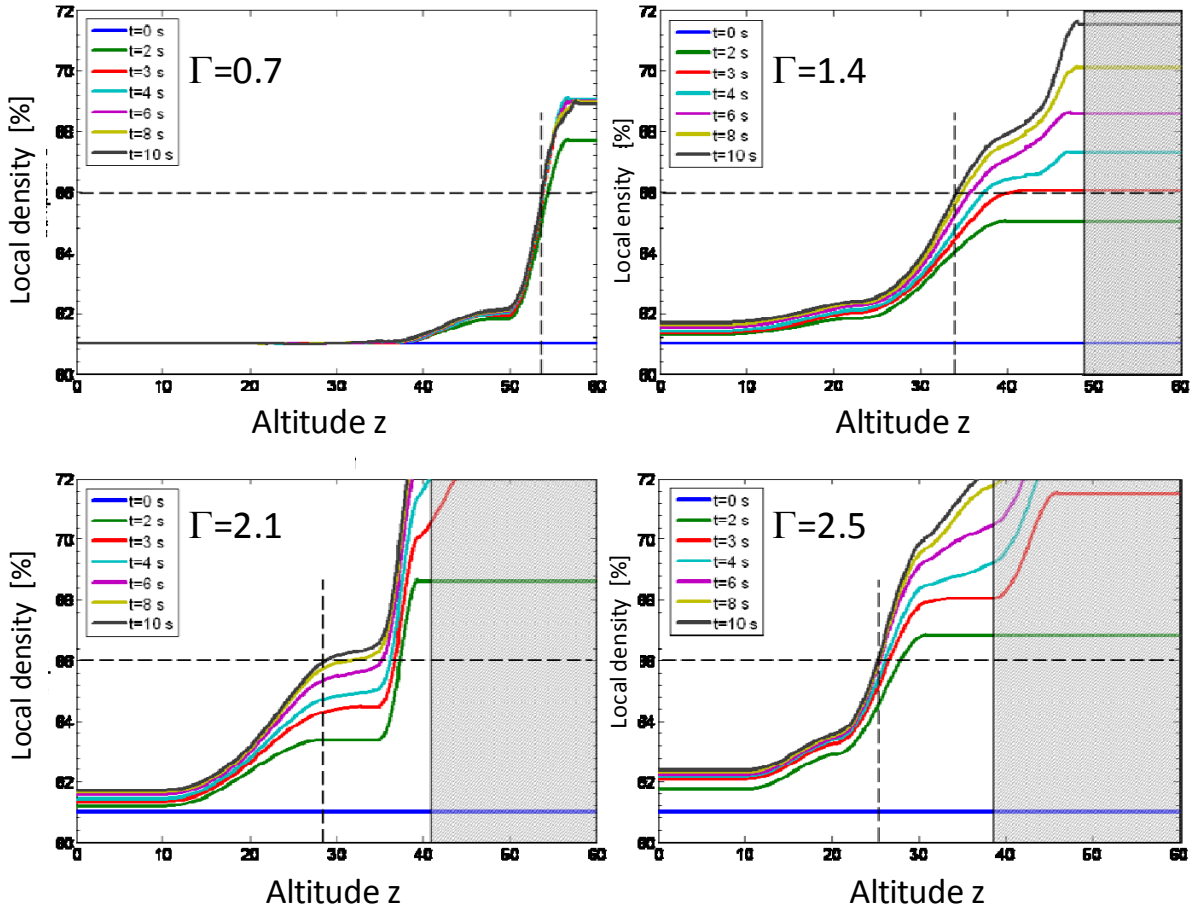

Figure 8: Evolution of the density profiles C(z) with time during the first 10 seconds for different accelerations Γ, in sand beds with initial density C_0=0.61. Systematic smoothing has been used in the calculations. The grey colored regions indicate the convective part of the samples, in which measurements cannot be performed. It can also be observed that unexpectedly large densities are obtained for altitudes z close to the convective region limit, showing that measurements are biased by the proximity of the convective rolls, which limits the accuracy of the method for high z values.

On the basis of these δz profiles, the density profiles (Figure 8) can be calculated from Equation 5. The profiles mainly evolve during the first 6 seconds, and then tend to be stabilized after 10 seconds. For large accelerations, a small homogeneous densification takes place in the bottom region (10 to 20 mm). The densification increases with altitude and acceleration, and a region of high density is observed. Abnormal values are however obtained when altitude is close to the limit of the convective region (Figure 8), which can be regarded as a limitation of the technique. The transition between the assumed (not densified) "jammed" and (highly densified) "glassy" regions presented in the introduction (Figure 1) is confirmed, but corresponds to region of rapidly evolving density, so that a conventional limit is to be defined. To evaluate the size and position of the highly densified region, an arbitrary density limit of 66% (2% below the expected maximum obtained by the rain-like technique) has been chosen as the limit of the highly densified region. The results plotted on Figure 9 show that a minimum acceleration (between 0.4 and 0.5) is needed to form the dense region. The highly compacted region moves downwards with increasing accelerations, and reaches the bottom of the sample at about Γ=3.

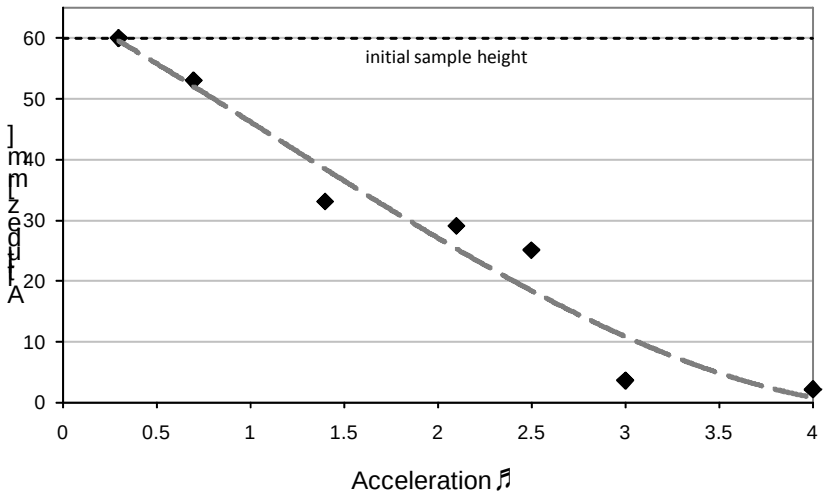

Figure 9: Position of the interface between upper compacted and lower not-yet-compacted regions as a function of the acceleration (threshold at 66% dynamic density). The position of the interface between the compacted region and convective rolls cannot be obtained from the present measurements.

Steady-state regime and relaxation

During the steady state regime, the overall shape of the packing remains constant and is not affected by the convective motion inside the sample. The corresponding density is called here the "dynamic" density of the sample. When vibrations are stopped the height of the sample decreases rapidly (Figure 10): the mean density increases. Since the solid-like bottom region has already been densified during the transient stage, the overall decrease of the packing height is mainly due to the relaxation in the fluidized region. This leads to the overall "relaxed" density.

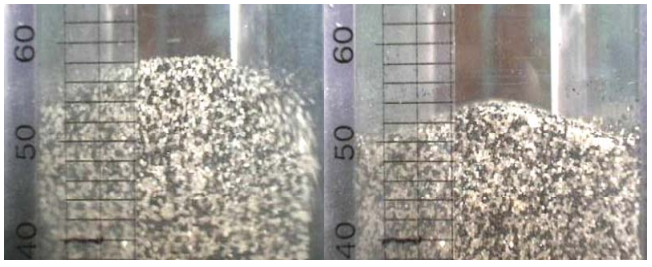

a b

Figure 10: West view of the upper part of a ~60 mm high sand packing: a) during vibration at f=50 Hz and Γ=6 ; b) after relaxation

The evolution of dynamic and relaxed densities measured by using the optical pen technique is reported on Figure 11 for a sample of height 60 mm. The dynamic and relaxed densities evolve in a similar way with acceleration, with a first increase up to about Γ=4, then a slight decrease for higher accelerations. The difference between the two densities is almost zero for accelerations below 1 and increases with acceleration. This is in agreement with the increase of the convective zone with acceleration and the assumption that relaxation mainly occurs in his region.

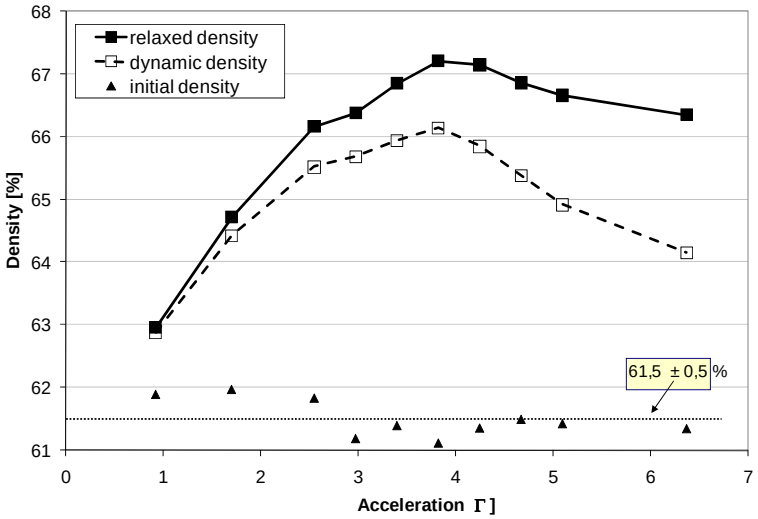

Figure 11: Evolution with acceleration of the dynamic and relaxed densities for a sample of height 60 mm. The corresponding initial density of each sample (0.61±0.05) is also reported.

Discussion

The curve of Figure 11 first shows an increase in density (typically starting around $\Gamma=\Gamma_0$), which is compatible with the dynamic height decrease observed during vibrations. For increasing accelerations, the relaxed density increases up to a maximum value for Γ around 4 then decreases to reach a stable value of about 0.66 for high accelerations. This value is slightly lower than the one we have obtained, when packing the same sand by the classic rain-like technique (around 0.68).

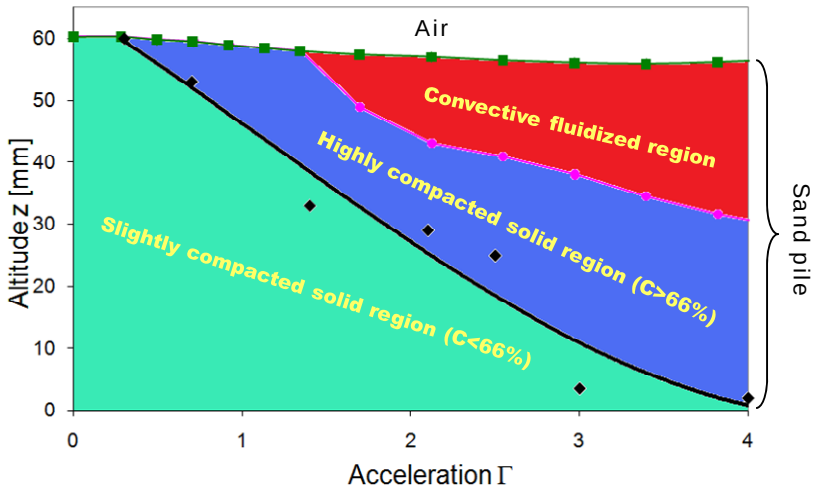

Figure 12: The dynamic regions of a sand sample of initial height 60 mm vs. acceleration for 50 Hz vibrations. The altitude is reported with respect to the initial position of the free surface (dotted line). The dashed line indicates where the bottom of a box filled with an initial height of 30 mm would be. (synthesis of the present results with references [13, 22, 24]).

The density maximum observed on Figure 11 is in agreement with dynamic observations if we consider the two phenomena:

- the expansion of the intermediate high density region, which tends to increase overall density in both dynamic and relaxed states. The densifying solid region is however limited by the bottom of the powder bed.
- the thickening of the fluidized top region with Γ, at the expense of the packed solid-like region. This phenomenon tends to decrease the dynamic density.

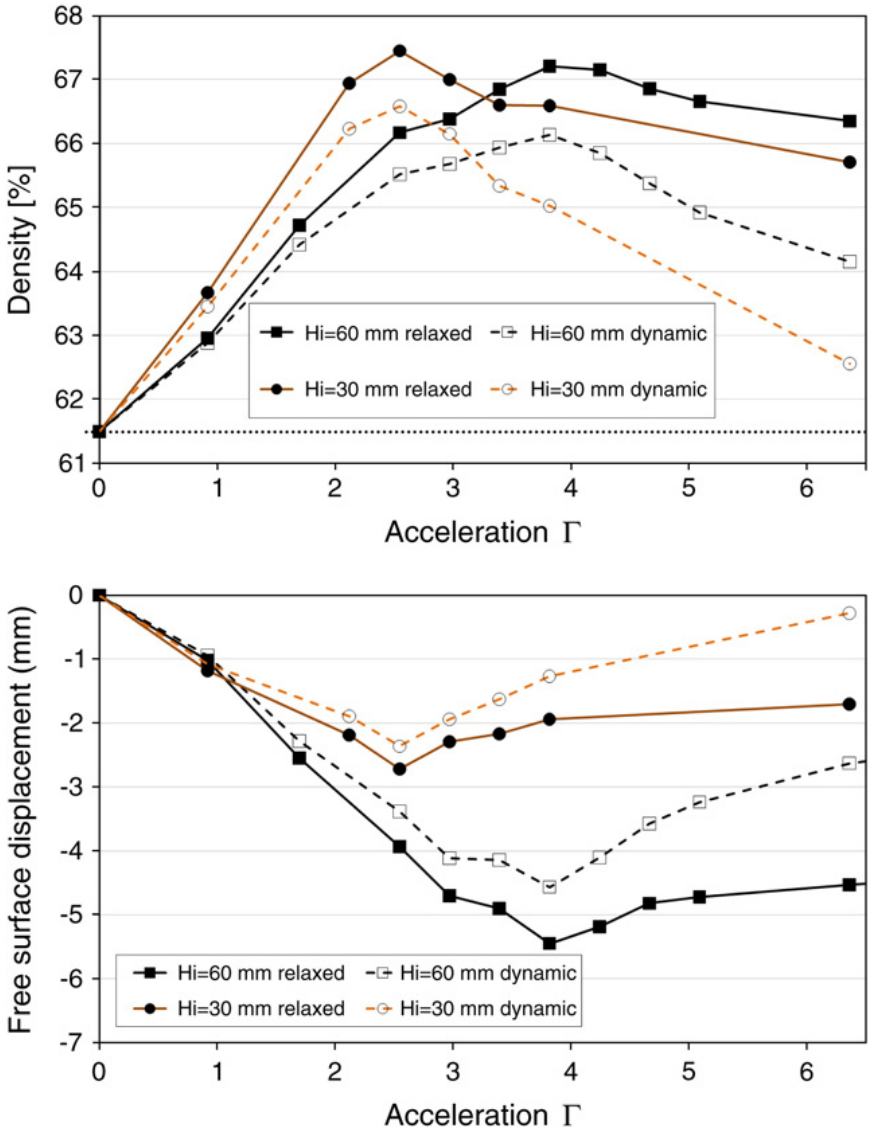

Figure 13: Evolution of densification with acceleration for two different initial sample heights H_i = 60 mm and H_i = 30 mm (f = 50 Hz). The initial density in all experiments is 61.5 ± 0.5%. a) Relaxed and dynamic density. b) Corresponding free surface displacement.

The compromise between the two tendencies leads to the observed maximum. When the acceleration is further increased, the expansion of the convective region corresponds to a decrease of the dynamic density. Relaxation of this fluidized region leads to a density lower than the solid vibrated one, which explains that the relaxed density slowly decreases after the maximum.

A slight densification occurs during vibrations even in the bottom of the sand bed. The main densification occurs in an intermediate region between the bottom and the upper fluidized region. The difference between relaxed and dynamic densities is associated to the relaxation of the fluidized region when vibration stops. If we associate the present results with the evaluation of the width of the fluidized zones measured from velocity fields [13, 22, 24], the schematic presentation of Figure 1 is confirmed and can be quantitatively drawn in the case of 60 mm high initial packings (Figure 11).

To present these results, obtained for a given initial sample height (60 mm), the distance z from the initial position of the surface was used, as the sample top is free and independent of the sample, while the bottom is constrained by the above layers. Because of these stress effects of the sand pile one can

expect a role of the initial height on the behaviour of the granular medium. Therefore, dynamic and relaxed densities of samples of 30 and 60 mm height respectively have been compared in Figure 13.

The first observation is that the maximum density is almost independent of the initial height. The second one is that there is a shift in the acceleration value at which the maximum density is reached (Figure 13a).

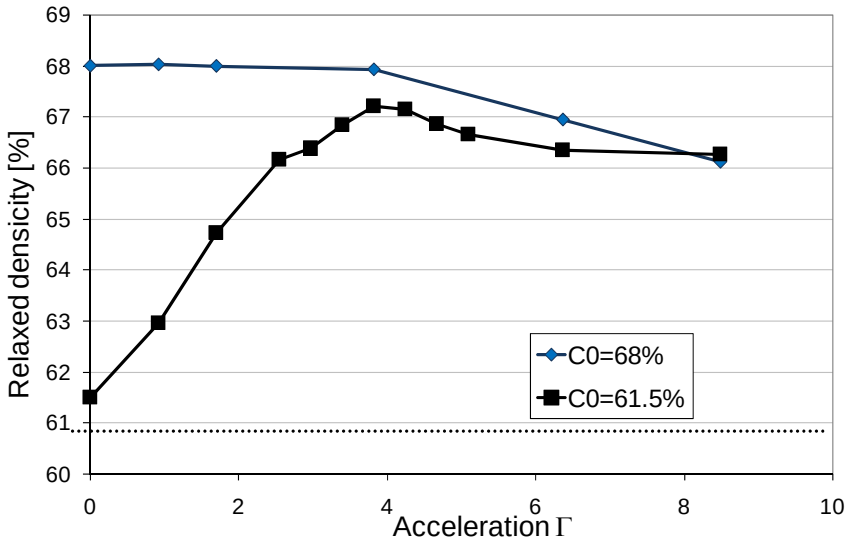

Figure 14: Comparison of the evolution of the relaxed density with acceleration for two initial densities C_0 of 61.5% and 68% (rain-like technique)

First let us notice that the thicknesses of the convective region and of the highly compacted region deduced from data given on Figure 11 are almost independent of the initial height.

If we consider the 30 mm sample, the maximum value is obtained for Γ about 2.5, which corresponds to a convective region of 15 mm (after Figure 11), and the highly densified region should be more than 30 mm below the surface. In other words, the densified region has reached the bottom: about half of the sample is highly densified, and half of the sample is involved in convective motion (Figure 12). The situation is almost the same if we consider the 60 mm sample at Γ around 4, which corresponds to the maximum densification. This interpretation "from the top of the sample" in agreement with the evolution of the free surface displacement in these samples (Figure 13b): the evolutions for 30 and 60 mm are the same for small accelerations and separate when Γ reaches values around 1.5 to 2, *i.e.*, when the compacted region reaches the bottom (Figure 12). It should of course be confirmed by complementary data on samples with different heights.

The value of the maximum relaxed density is slightly below the maximum of 68% obtained by rain-like techniques. Experiments using such high density samples (Figure 14) show that in this case, after a plateau the relaxed density decreases with acceleration for Γ > 4. Relaxation of fluidized regions in this range of acceleration does not allow to reaching the maximum 68% relaxed density. Note that the depth of the fluidized region is expected to depend very weakly on initial density.

Conclusions

The use of two techniques gives complementary information that is helpful to describe the densification phenomenon observed in a horizontally vibrated sand pile. The influence of the acceleration on the global dynamic (steady state) and relaxed densities is studied. It appears that the densification is maximal for a critical acceleration value, depending on the initial packing height (Γmax = 3.8 for Hi = 60 mm). The study of the transient regime (the first 10 s) allows us to propose an explanation for the shape of the curve C = f(Γ). The latter is shown to be related to the existence of three regions inside the vibrated bed (a slightly compacted lower layer, a highly compacted intermediate layer and a convective fluidized upper layer) as well as the evolution of their thickness as a function of the acceleration.

An important limitation of the present work is the assumption that the measurements performed at the surface can be quantitatively used to describe the phenomena inside the sample. Two ways are presently investigated to check this hypothesis. The first one is to perform an *a posteriori* control of

these results by analyzing the final structure with 3D X-ray tomography. The second one is to numerically study the grains movements during vibrations with a Discrete Elements Method simulation software. First results have already been obtained in this field [26].

Acknowledgments

We wish to thank A. Belhaoua, Johan Debayle and Jean-Charles Pinoli (Ecole des Mines, CIS Center), who designed the method and wrote the software for computing the velocity field: their contribution was quite essential to enable this work, and Albert Boyer for its technical support.

References

[1] K.M . Aoki, T.Akiyama, Y.J.Maki and T. Watanabe, Convective roll patterns in vertically vibrated beds of granules. Phys. Rev. E, (1996) 54(1): pp. 874–883

[2] S.McNamara and S. Luding. Energy flows in vibrated granular media. Physical Review E, (1998) 58(1): pp. 813–822.

[3] S. Fauve, S. Douady and C. Laroche. Collective Behaviors of Granular Masses under Vertical Vibrations. Journal De Physique, (1989) 50(C-3): pp. 187-191.

[4] J.B. Knight, E.E. Ehrichs, V.Y. Kuperman, J.K.Flint, H.M.Jaeger, and S.R.Nagel, Experimental study of granular convection. Physical Review E, (1996) 54(5): pp. 5726-5738.

[5] S.S., Hsiau, P.C. Wang and C.H. Tai. Convection cells and segregation in a vibrated granular bed. AIChE Journal, (2002) 48(7): pp.1430–1438.

[6] E. Rouèche, G. Thomas, J.L. Gelet, J.M. Missiaen. Dependence of granular arrangements under vibrations on the dimensions of cylindrical containers. Powder & Grains, Vol. 2, Ed. R. Gardia-Rojo, H.J. Herrmann and S. Mc Namara, Balkema (2005), pp. 1177-1180.

[7] S.S. Hsiau, M.Y. Ou and C.H. Tai. The flow beh*a*vior of granular material due to horizontal shaking. Advanced Powder Technology, (2002) 13(2) pp. 167-180.

[8] K. Liffman, G. Metcalfe and P. Cleary. Granular convection and transport due to horizontal shaking. Physical Review Letters, (1997) 79(23): pp. 4574-4576.

[9] C. Salueña and T. Poschel. Convection in horizontally shaken granular material. European Physical Journal E, (2000) 1(1): pp. 55-59.

[10] S.G.K. Tennakoon, L. Kondic and R.P. Behringer. Onset of flow in a horizontally vibrated granular bed : Convection by horizontal shearing. Europhysics Letters, (1999) 45(4): pp. 470-475.

[11] G. Metcalfe, S.G.K. Tennakoon, L. Kondic, D.G. Schaeffer and R.P. Behringer. Granular friction, Coulomb failure, and the fluid-solid transition for horizontally shaken granular materials. Physical Review E, (2002) 65(3): Art. N°031302

[12] M. Medved, D. Dawson, H.M. Jaeger and S.R. Nagel. Convection in horizontally vibrated granular material. Chaos, (1999) 9(3): pp. 691-696.

[13] A. Raihane, O. Bonnefoy, J.-L. Gelet, J.-M. Chaix and G. Thomas. Experimental study of a 3D dry granular medium submitted to horizontal shaking, Powder Technology, (2009) 190: pp. 252–257

[14] S. Aumaitre, C. Puls, J.N. McElwaine, J.P. Gollub. Comparing flow thresholds and dynamics for oscillating and inclined granular layers. Physical Review E, (2007) 061307-1–061307-9

[15] R.C.Flemmer, I.J., Yule. Coherence of a packed bed under lateral oscillation, Powder Technol., (2007) 171: pp. 154-156

[16] A. Kudrolli, Size separation in vibrated granular matter. Rp. Prog. Phys., (2004) 67: pp.209-247.

[17] T. H. Metcalf, J. B. Knight and H. M. Jaeger. Standing wave patterns in shallow beds of vibrated granular material Physica A, (1997) A 236 (3-4) : pp. 202-210.

[18] F. Melo, P. Umbanhowar and H. L. Swinney. Transition to parametric wave patterns in a vertically oscillated granular layer. Phys. Rev. Lett., (1994) 72: pp. 172-175.

[19] I.S. Aranson, L.S. Tsimring. Patterns and collective behaviour in granular media: theoretical concepts. REV; Modern Physics, (2006) 78: pp. 641-691

[20] E. R. Nowak, J. B. Knight, E. Ben-Naim, H. M. Jaeger and S. R. Nagel, Phys. Rev., (1998) E 57: pp. 1971-1982.

[21] P. Richard, P. Philippe, F. Barbe, S. Bourlès, X. Thibault and D. Bideau, Phys. Rev. E, (2003) 68, Art. N°020301.

[22] A. Raihane, O. Bonnefoy, J-L. Gelet, J-M. Chaix and G. Thomas. Densification of a 3D granular bed by horizontal vibrations, Proceedings of the XVth International Congress on Rheology (ICR2008) August 3-8, 2008, Monterey, California, USA. American Institute of Physics Conference Proceedings vol. 1027, ISBN: 978-0-7354-0550-9, pp. 932-935.

[23] Evesque P., Fargeix D., Habib P, Luong M.P., Porion P., "Pile density is a control parameter of sand avalanches", Phys. Rev. E, (1993) 47(4): pp. 2326-2332.

[24] A. Raihane, O. Bonnefoy, , J-L. Gelet, J-M. Chaix et G. Thomas. Convective flow in a horizontally vibrated 3D granular packing, Powders & Grains 2009, July 13-17, 2009, Colorado, USA, 721-724.

[25] J. Debayle, A. Raihane, A. Belhaoua, O. Bonnefoy, G. Thomas, J.M. Chaix and J-C. Pinoli, Velocity field computation in vibrated granular media using an optical flow based multiscale image analysis method, Image Anal. Stereol., (2009) 28: pp.35-43

[26] S. Nadler, O. Bonnefoy, A. Raihane, J-L. Gelet, J-M. Chaix et G. Thomas. Numerical simulation of granular media under horizontal vibration. Powders&Grains 2009, July 13-17, 2009, Colorado, USA, 725-728.